

Cite this: DOI: 10.1039/xxxxxxxxxx

## Probabilistic determination of the effect of a deep-eutectic solvent on the structure of lipid monolayers

Adrian Sanchez-Fernandez,<sup>ab†</sup> Andrew R. McCluskey,<sup>ac†</sup> Karen J. Edler,<sup>\*a†</sup> Andrew J. Jackson,<sup>bd</sup> Richard A. Campbell,<sup>e</sup> and Thomas Arnold<sup>abc</sup>

Received Date

Accepted Date

DOI: 10.1039/xxxxxxxxxx

www.rsc.org/journalname

The abstract should be a single paragraph which summarises the content of the article. Any references in the abstract should be written out in full e.g. [Surname *et al.*, *Journal Title*, 2000, **35**, 3523].

### Introduction

Deep eutectic solvents (DES) are green, sustainable solvents obtained through the complexation of naturally occurring compounds, such as sugars, alcohols, amines and carboxylic acids, among others.<sup>1,2</sup> An extensive hydrogen-bonding network is present between the precursors, allowing the mixture to remain liquid at room temperature due to the high-entropy state of the mixture.<sup>3–5</sup> Furthermore, through different combinations of the precursors materials, it is possible to tune the physicochemical properties of the solvent, such as polarity,<sup>6</sup> viscosity and surface tension,<sup>1</sup> network charge,<sup>7</sup> and hydrophobicity.<sup>8,9</sup>

These solvents have recently shown the ability to promote the self-assembly of surfactants into micellar structures<sup>10,11</sup> and to stabilise the conformation of non-ionic polymer species,<sup>12</sup> demonstrating the presence of a solvophobic effect. The behaviour of biomolecules in DES has also seen an increase in interest, due to potential applications towards the preservation of biomolecules by DES, and as environments for enzymatic reactions<sup>13</sup> additionally, the behaviour and conformation of proteins and enzymes in these solvents have received remarkable interest.<sup>14–21</sup> Finally, recent investigations have also shown that DES have been shown to support the formation of phospholipid bilayers.<sup>22–24</sup>

The formation of phospholipid monolayers plays a key role in

many biological and technological processes. The amphiphilic lipids commonly show a low solubility in one of the two phases, leading to the formation of a stable monolayer at the interface.<sup>25</sup> Phospholipid consist of a charged headgroup, either anionic or zwitterionic, and investigations at the air-salt water interface have revealed the importance of the lipid-ion interactions on structure, monomer packing and stability of the monolayer.<sup>25,26</sup> Despite the broad interest in these systems, the presence of stable phospholipid monolayers in non-aqueous media has not been reported, to the best of the authors' knowledge.

Recent developments in computational resources and software has enabled powerful methodologies to be harnessed by those from non-computer science backgrounds. This has mostly occurred through open-source software projects such as Python and the Jupyter notebooks framework.<sup>27,28</sup> In the area of neutron and X-ray reflectometry data-analysis, this has led to the development of tool such as refnx,<sup>29</sup> a Python library for the fitting of layer-based models to reflectometry data. The availability of such software enables the use of models that contain chemical-context within their structure. Wherein, the chemically-relevant information known about the system is used within the model, such as the constraint that the number density of phospholipid headgroups must be the same as the number density of pairs of phospholipid tailgroups.

The use of a Python library for fitting enable powerful probability distribution function sampling methods to be used such as the Goodman & Weare Affine Invariant Markov chain Monte Carlo (MCMC) Ensemble,<sup>30</sup> as implemented in the Python library emcee.<sup>31</sup> This library allows for the sampling of a high-dimensionality parameter space, such as that which is relevant to reflectometry fitting to be performed with relative ease. This results in estimations of the inverse uncertainties associated with each parameter as well as information about the correlations between different parameters within the model.

In this work, we present the first investigation of the structure of phospholipid monolayers at the air-DES inter-

<sup>a</sup> Department of Chemistry, University of Bath, Claverton Down, Bath, BA2 7AY, UK.

<sup>b</sup> European Spallation Source, SE-211 00 Lund, Sweden.

<sup>c</sup> Diamond Light Source, Harwell Campus, Didcot, OX11 0DE, UK.

<sup>d</sup> Department of Physical Chemistry, Lund University, SE-211 00 Lund, Sweden.

<sup>e</sup> Institut Laue-Langevin, 71 avenue des Martyrs, 38000, Grenoble, France.

<sup>†</sup> These authors have contributed equally to the work presented here.

\* Corresponding author: k.edler@bath.ac.uk

† Electronic Supplementary Information (ESI) available: [details of any supplementary information available should be included here]. See DOI: 10.1039/b000000x/

‡ Additional footnotes to the title and authors can be included e.g. 'Present address:' or 'These authors contributed equally to this work' as above using the symbols: ‡, §, and ¶. Please place the appropriate symbol next to the author's name and include a \footnotetext entry in the correct place in the list.

face, as determined by chemical-context modelling of X-ray reflectometry measurements. Four different phospholipids; 1,2-dipalmitoyl-sn-glycero-3-phosphocholine (DPPC), 1,2-dimyristoyl-sn-glycero-3-phosphocholine (DMPC), 1,2-dilauroyl-sn-glycero-3-phosphocholine (DLPC) and 1,2-dimyristoyl-sn-glycero-3-phospho-(1'-rac-glycerol) (DMPG), were studied at the interface between a 1:2 mixture of choline chloride:glycerol and air. This allowed the nature of two, chemically distinct, phospholipid headgroups to be understood in this non-aqueous solvent, in addition to the effect of the tail chain length.

## Experimental

### Materials

Choline chloride (99 %, Sigma-Aldrich) and glycerol (99 %, Sigma-Aldrich) were purchased and used without further purification. The deep eutectic solvent was prepared by mixing the precursors at the appropriate mole ratio, and heating at 80 °C until a homogeneous, transparent liquid was formed.<sup>1</sup> The solvent was equilibrated overnight at 40 °C and subsequently stored under a dry atmosphere.

The water content on the deep eutectic solvent was determined before and after each experiment by Karl-Fischer titration (Mettler Toledo DL32 Karl-Fischer Coulometer, Aqualine Electrolyte A, Aqualine Catholyte CG A) in order to keep track of any effect from the presence of water on our results. Those measurements showed that the water content of the solvent was kept below 0.3 wt% during all the experimental procedures presented here, which we assume to be negligible and have little impact on the characteristics of the DES.<sup>3,4</sup>

DPPC (> 99 %), DMPC (> 99 %), and DMPG (> 99 %) were supplied by Avanti Polar Lipids and used as received. DLPC (> 99 %) was supplied by Sigma-Aldrich and used as received. Sample preparation was performed *in situ* using the standard method for the spreading of insoluble monolayers on water: a certain amount of the phospholipid solution was spread onto the liquid surface in order to provide a given surface concentration. After the evaporation of the chloroform, it is assumed that the resulting system is a solvent subphase with a monolayer of phospholipid at the interface. Surface concentration was modified by closing and opening the PTFE barriers of the Langmuir trough (XRR).

### Methods

X-ray reflectivity measurements were taken on I07 at Diamond Light Source, at 12.5 keV photon energy using the double-crystal-deflector.<sup>32</sup> The reflected intensity was measured in a momentum transfer range from 0.018 to 0.7 Å<sup>-1</sup>. The data was normalised to the incident beam and background was measured from off-specular reflection and subsequently subtracted. The sample environment consisted of a PTFE Langmuir trough. Samples were equilibrated for at least one hour and preserved under argon atmosphere to minimise the adsorption of water by the subphase. Surface concentration was controlled through opening and closing the barriers of the Langmuir trough and measured using an aluminium Wilhelmy plate. X-ray reflectivity data were collected for each of the lipids, DMPC, DPPC, DLPC and DMPG and all

measurements were made at 22 °C at five different surface concentrations.

### Data analysis

The use of reflectometry to analyse the structure of phospholipids on the surface of water has a history extending over many years.<sup>25,26,33–37</sup> This has led to some variation in the models used to fit experimental data, shown in Table 1. Although, there appears to be a general consensus that the molecular volume of the phosphocholine is in the region of 320 Å<sup>3</sup>, and as a result this figure is also used as a physical constraint on the layer model when fitting reflectometry data. However, as this work involves the use of a non-aqueous solvent system we believe that the literature values for the head group molecular volumes may be unreliable. This is due to the charged nature of the zwitterionic and anionic lipid heads having a significant interaction with the solvent in both the neutral water and the charged DES.

To allow for the use of a chemically-relevant model, where the lipid head group molecular volume was allowed to vary, the Python library `refnx`<sup>29</sup> as used. This software allows the inclusion of a custom chemically-sensible model from which the parameters to be fed into the Abelès layer-model,<sup>46,47</sup> that is typical for reflectometry fitting, are obtained. This custom model, along with Jupyter notebook showing in full the analysis performed, can be found in the ESI.

This chemical model involves considering the lipids as consisting of head groups and tail groups. The head groups have a calculated scattering length,  $b_h$ , (found as a summation of the number of electrons in the head group multiplied by the classical radius of the electron), and a molecular volume,  $V_h$ . The head groups make up a layer with a given thickness,  $d_h$ , and roughness,  $\sigma_h$ , with a same volume fraction of solvent can intercalate into the head group region,  $\phi_h$ . While, the tail groups also have a calculated scattering length,  $b_t$ , and molecular volume,  $V_t$ , however the thickness of the tail group layer,  $d_t$ , is found from the length of the carbon tail,  $t_t$ , and angle that the chain is tilted by with respect to the interface normal,  $\theta_t$ ,

$$d_t = t_t \cos \theta_t. \quad (1)$$

The air above the monolayer is also able to solvate the tail region with some volume fraction,  $\phi_t$ . The scattering length density of the tail and head layers used in the Abelès model can therefore be found as follows,

$$\text{SLD}_i = \frac{b_i}{V_i} (1 - \phi_i) + \text{SLD}_s \phi_i, \quad (2)$$

where  $\text{SLD}_s$  is the scattering length density of the superphase (air) and the subphase (DES) for the tail and head groups respectively, and  $i$  indicates either the tail or head layer. In order to ensure that the number density of head groups and pairs of tail groups is the same, the following constraint was added to the model,

$$d_h = \frac{V_h d_t (1 - \phi_t)}{V_t (1 - \phi_h)}. \quad (3)$$

This custom model was used to co-refine the two highest sur-

**Table 1** Lipid component volumes extracted from different literature sources.  $V_t$  corresponds to the total lipid volume, MD to molecular dynamics simulation, WAXS to wide-angle X-ray scattering, NB to neutral buoyancy and DVTS to differential vibrating tube densimetry

Lipid	DPPC			DMPC			DMPG
Reference	[38]	[39]	[40]	[41]	[42]	[43]	[45]
$V_t/\text{\AA}^3$	1216.96	1219	1148	1224	1101	1061	1094
$V_h/\text{\AA}^3$	326.00	324	319	360	319	344	291
$V_i/\text{\AA}^3$	890.96	895	829	864	782	717	767
Method	MD	MD	WAXS	NB	NB	NB	DVTS
T/°C	25	50	24	25	30	30	DVTS

face concentration measurements to determine the molecular volume for the lipid head group,  $V_h$ , which was allowed to vary within reasonable bounds but held constant between the two concentrations. Other parameters that were allowed to vary were  $\theta_t$ ,  $\phi_t$ ,  $\phi_h$ ,  $\sigma_t$ , and  $\sigma_h$ , while the parameters shown in Table 2 were held constant at the values given. The length of the carbon chain was kept constant to the value given by the Tanford equation,<sup>48</sup> this is valid due to the condensed nature of the monolayer at this surface pressure resulting in the extending, staggered conformation of the chain being likely.

**Table 2** The variant parameters within the chemically-sensible model.  
<sup>a</sup>Values determined from Armen *et al.*<sup>38</sup> <sup>b</sup>Values obtained from the Tanford formula where the carbon chains are assumed to be fully extended.<sup>48</sup> <sup>c</sup>Values extracted from Sanchez-Fernandez *et al.*<sup>10</sup>

Parameter	Value
DP- $b_t/\text{fm}$	6897
DM- $b_t/\text{fm}$	5985
DL- $b_t/\text{fm}$	5073
PC- $b_h/\text{fm}$	4674
PG- $b_h/\text{fm}$	4731
DP- $V_t/\text{\AA}^3$	891 <sup>a</sup>
DM- $V_t/\text{\AA}^3$	779 <sup>a</sup>
DL- $V_t/\text{\AA}^3$	667 <sup>a</sup>
DP- $t_t/\text{\AA}$	21.8 <sup>b</sup>
DM- $t_t/\text{\AA}$	19.3 <sup>b</sup>
DL- $t_t/\text{\AA}$	16.7 <sup>b</sup>
SLD <sub>sup</sub> /×10 <sup>-6</sup> $\text{\AA}^{-2}$	0
SLD <sub>sub</sub> /×10 <sup>-6</sup> $\text{\AA}^{-2}$	10.8 <sup>c</sup>

The fitting of the reflectometry model to the experimental involved transforming the result of the model and the data into  $rq^4$  such that the artifact of the Fresnel decay was removed before using the differential evolution method available to refnx from the scipy library, to find the parameters which gave the best fit to the data. The parameter space for each of these was then probed using the MCMC method available through emcee, this allowed for an estimate of the probability distribution function associated with each parameter. In the MCMC sampling, 200 walkers were used over 1000 iterations, following an equilibration of 200 iterations.

## Results & Discussion

The custom model with a variable head molecular volume, was co-refined for the highest two concentrations of all lipids. The resulting reflectometry profiles, associated scattering length density profiles and the probability distribution function (PDF) for the head group molecular volume are shown in Figure 1. Table 3 gives details of the other varying parameters for each lipid, these

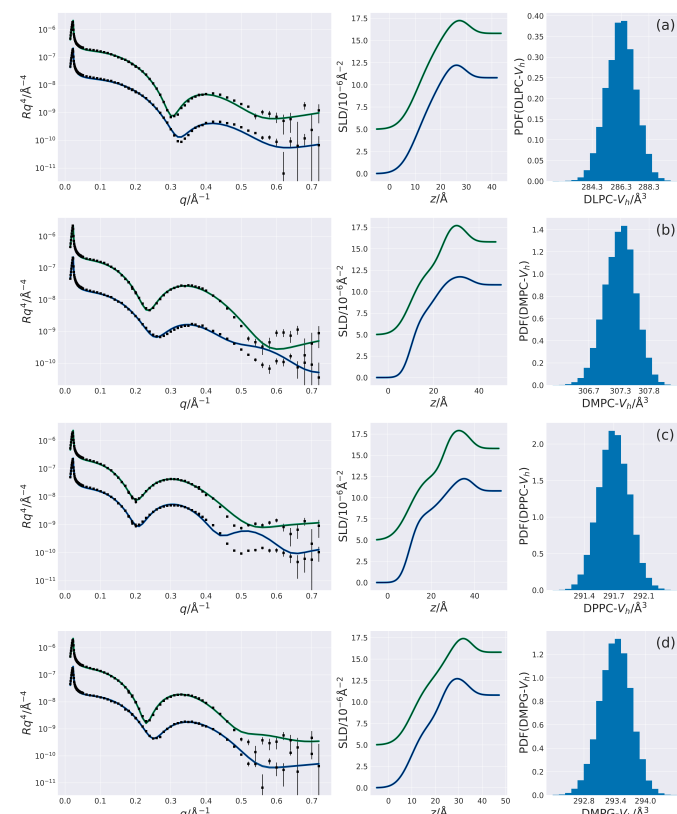


**Fig. 1** The reflectometry profile, scattering length density profile and probability distribution function for each of the three phosphocholine containing lipids; (a) DLPC, (b) DMPC, (c) DPPC, (d) DMPG.

are given with asymmetric error bars which give the 95 % confidence interval, the full probability distribution plots can be found in the ESI.

Since the tail chain length is held constant to the value of the Tanford length for a given lipid tail, there is a direct correlation between the thickness of the tail layer and the chain tilt angle from the model. It can be seen from Table 3 that as would be expected, and as found in previous work,<sup>25,49</sup> the thickness of the tail layer increases as the number of carbon atoms in the tail chains increases. Additionally, it is also observed that the value of the chain tilt either decreases, resulting in a tail thickness increase, or remains constant as the surface concentration increases. This indicates that for DLPC and DPPC these two highest surface concentration measurements were at a similar area per molecule, while the area per molecule slightly decreased between the two measurements for DMPC and DPPC. The phenomena of the tail thickness increasing with increasing surface pressure has been noted before for DMPC at the air-water interface.<sup>50</sup> Furthermore, as the surface concentration increases, the amount of solvent in the head layer decreases, or stays the same, as would be expected with the head layer becoming more packed and therefore there is less space for solvent.

The thickness of the tail layers in these condensed monolayers appears to agree well with values found for water-analogues for each of the lipids (DMPC:  $d_t = 15.8 \text{ \AA}$ ,<sup>34</sup> DPPC:  $d_t = 16.7 \text{ \AA}$ <sup>36</sup>). Previous work indicates, although there has been no direct comparison that the phosphatidylglycerol head layer may be thicker than phosphocholine at a water-air interface.<sup>34,35,49,50</sup> However, the phosphocholine head group appears to be slightly expanded in the DES compared to in water (PPC:  $d_h = 8.4 \text{ \AA}$ <sup>36</sup>) resulting in the values for the thicknesses of the head layers being similar between the two head groups.

Figures 1(a-c) shows the PDF determined for the head group volume for each of the four lipids. The three lipids with a phosphocholine head group appear to show some unsystematic variance with values of  $286.34^{+2.03}_{-1.94} \text{ \AA}^3$  for DLPC,  $307.28^{+0.57}_{-0.51} \text{ \AA}^3$  for DMPC, and  $291.73^{+0.35}_{-0.35} \text{ \AA}^3$  for DPPC. This is significantly less than the largest estimate of the head volume from literature sources,  $360 \text{ \AA}^3$ ,<sup>41</sup> and slightly less than lowest estimate,  $319 \text{ \AA}^3$ .<sup>40,42</sup> The fact that the choline chloride component of the DES is charged in nature suggests that it has a screening effect on the charged interactions between the zwitterionic phosphocholine head groups reducing the volume that it occupies.

Figure 1(d) contains the PDF for the phosphatidylglycerol head group volume, which was found to be  $293.43^{+0.59}_{-0.55} \text{ \AA}^3$ . This agrees well with the literature value for this lipid head group of  $291 \text{ \AA}^3$ ,<sup>45</sup> indicating that the charged component of the DES solvent has little affect on the volume occupied by the phosphatidylglycerol head group.

It is possible to generalise the difference between the two lipid head groups in terms of the difference in their charges, with the phosphocholine group being zwitterionic in nature while the phosphatidylglycerol is anionic (Figure 2). The fact that the phosphatidylglycerol head group appears to show no deviation in volume at the air-DES interface, when compared with the air-

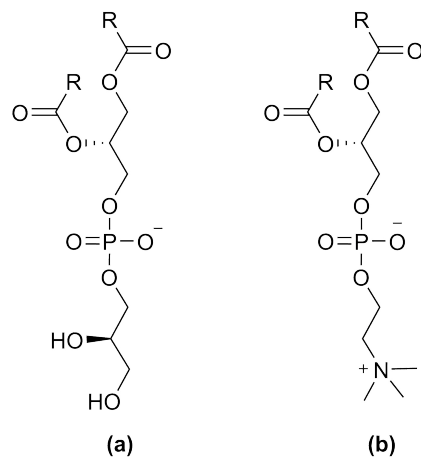


**Fig. 2** The two lipid head groups compared in this study, where R indicates the carbon tail; (a) phosphatidylglycerol, (b) phosphocholine.

water interface, suggests that the interaction resulting in the apparent decrease in volume of the phosphocholine head group is due to the positively-charged nitrogen group interacting with the negatively-charged chloride component of the DES. The relatively small size of the chloride ion, compared to the choline moiety, means that it is able to intercalate more easily into the lipid head layer allowing for the charge screening to occur.

Previous work has suggested that the DES may provide a segregated environment to better solubilise the phospholipid head groups.<sup>22,23</sup> Since both the phosphatidylglycerol and phosphocholine head groups contain a moiety of the DES solvent, it is possible for the choline terminal of the phosphocholine would favour the presence of glycerol, while the glycerol terminal of the phosphatidylglycerol would be favourable solubilised by the choline moiety of the DES. This solvent segregation of the DES may result in the phosphocholine head group being preferentially solubilised due to the greater molar abundance of glycerol in the 1:2 mixture, and hence giving a smaller volume for this head group than found in water.

## Conclusions

The conclusions section should come in this section at the end of the article, before the Conflicts of interest statement.

## Conflicts of interest

There are no conflicts to declare.

## Acknowledgements

The authors would like to thank the European Spallation Source and the University of Bath Alumni Fund for supporting A.S.-F. A.R.M. is grateful to the university of Bath and Diamond Light Source for co-funding a studentship (Studentship Number STU0149). We also thank Diamond Light Source and Institute Laue-Langevin for the awarded beamtime (SI10546-1 and 9-13-612 respectively).

**Table 3** The best-fit values, and associated 95 % confidence intervals for the varying parameters in the phosphocholine reflectometry model. The values of  $d_t$  were found from the appropriate values of  $\theta_t$  using Eqn. 1.

Parameter	DLPC		DMPC		DPPC		DMPG	
	Conc 4	Conc 5						
$\theta_t/^\circ$	46.62 <sup>+0.33</sup> <sub>-0.33</sub>	45.01 <sup>+0.30</sup> <sub>-0.30</sub>	52.26 <sup>+0.07</sup> <sub>-0.07</sub>	38.82 <sup>+0.23</sup> <sub>-0.27</sub>	34.54 <sup>+0.17</sup> <sub>-0.17</sub>	37.89 <sup>+0.09</sup> <sub>-0.10</sub>	45.06 <sup>+0.12</sup> <sub>-0.15</sub>	27.48 <sup>+0.42</sup> <sub>-0.42</sub>
$d_t/\text{\AA}$	10.61 <sup>+0.06</sup> <sub>-0.06</sub>	10.93 <sup>+0.06</sup> <sub>-0.06</sub>	10.61 <sup>+0.06</sup> <sub>-0.06</sub>	14.01 <sup>+0.05</sup> <sub>-0.05</sub>	16.90 <sup>+0.03</sup> <sub>-0.03</sub>	16.19 <sup>+0.02</sup> <sub>-0.02</sub>	12.70 <sup>+0.03</sup> <sub>-0.03</sub>	15.96 <sup>+0.06</sup> <sub>-0.06</sub>
$d_h/\text{\AA}$	8.11 <sup>+0.09</sup> <sub>-0.09</sub>	9.34 <sup>+0.08</sup> <sub>-0.09</sub>	8.11 <sup>+0.09</sup> <sub>-0.09</sub>	10.12 <sup>+0.13</sup> <sub>-0.12</sub>	11.92 <sup>+0.05</sup> <sub>-0.05</sub>	11.58 <sup>+0.06</sup> <sub>-0.06</sub>	11.27 <sup>+0.10</sup> <sub>-0.09</sub>	8.84 <sup>+0.07</sup> <sub>-0.07</sub>
$\phi_t \times 10^{-2}$	0.15 <sup>+0.14</sup> <sub>-0.54</sub>	0.05 <sup>+0.04</sup> <sub>-0.19</sub>	10.20 <sup>+0.34</sup> <sub>-0.34</sub>	0.05 <sup>+0.05</sup> <sub>-0.22</sub>	0.00 <sup>+0.00</sup> <sub>-0.02</sub>	0.00 <sup>+0.00</sup> <sub>-0.02</sub>	0.01 <sup>+0.01</sup> <sub>-0.07</sub>	6.32 <sup>+0.41</sup> <sub>-0.41</sub>
$\phi_h \times 10^{-2}$	43.88 <sup>+1.06</sup> <sub>-1.16</sub>	49.82 <sup>+0.71</sup> <sub>-0.74</sub>	74.63 <sup>+0.21</sup> <sub>-0.21</sub>	45.43 <sup>+0.88</sup> <sub>-0.79</sub>	53.60 <sup>+0.30</sup> <sub>-0.30</sub>	54.24 <sup>+0.31</sup> <sub>-0.29</sub>	57.54 <sup>+0.47</sup> <sub>-0.42</sub>	36.32 <sup>+0.95</sup> <sub>-0.95</sub>
$\sigma_t/\text{\AA}$	5.06 <sup>+0.03</sup> <sub>-0.03</sub>	5.19 <sup>+0.03</sup> <sub>-0.03</sub>	3.34 <sup>+0.01</sup> <sub>-0.01</sub>	5.20 <sup>+0.01</sup> <sub>-0.01</sub>	3.48 <sup>+0.00</sup> <sub>-0.00</sub>	5.94 <sup>+0.01</sup> <sub>-0.01</sub>	5.08 <sup>+0.01</sup> <sub>-0.01</sub>	5.33 <sup>+0.02</sup> <sub>-0.02</sub>
$\sigma_h/\text{\AA}$	5.57 <sup>+0.09</sup> <sub>-0.09</sub>	5.88 <sup>+0.10</sup> <sub>-0.10</sub>	5.20 <sup>+0.03</sup> <sub>-0.03</sub>	3.59 <sup>+0.05</sup> <sub>-0.06</sub>	7.07 <sup>+0.02</sup> <sub>-0.02</sub>	3.30 <sup>+0.02</sup> <sub>-0.02</sub>	3.56 <sup>+0.04</sup> <sub>-0.05</sub>	6.15 <sup>+0.04</sup> <sub>-0.04</sub>

## Notes and references

- E. L. Smith, A. P. Abbott and K. S. Ryder, *Chem. Rev.*, 2014, **114**, 11060–11082.
- Y. Dai, J. van Spronsen, G. J. Witkamp, R. Verpoorte and Y. H. Choi, *Anal. Chim. Acta.*, 2013, **766**, 61–68.
- O. S. Hammond, D. T. Bowron and K. J. Edler, *Green Chem.*, 2016, **18**, 2736–2744.
- O. S. Hammond, D. T. Bowron, A. J. Jackson, T. Arnold, A. Sanchez-Fernandez, N. Tsapataris, V. G. Sakai and K. J. Edler, *J. Phys. Chem.*, 2017, **121**, 7473–7483.
- C. F. Araujo, J. A. P. Coutinho, M. M. Nolasco, S. F. Parker, P. J. A. Ribeiro-Claro, S. Rudic, B. I. G. Soares and P. D. Vaz, *Phys. Chem. Chem. Phys.*, 2017, **19**, 17998–18009.
- A. Pandey, R. Rai, M. Pal and S. Pandey, *Phys. Chem. Chem. Phys.*, 2014, **16**, 1559–1568.
- S. Zahn, B. Kirchner and D. Mollenhauser, *Chem. Phys. Chem.*, 2016, **17**, 3354–3358.
- B. D. Ribeiro, C. Florindo, L. C. Iff, A. Z. Coelho and I. M. Marrucho, *ACS Sustain. Chem. Eng.*, 2015, **3**, 2469–2477.
- D. J. G. P. van Osch, L. F. Zubeir, A. van der Bruinhorst, M. A. A. Rocha and M. C. Kroon, *Green Chem.*, 2015, **17**, 4518–4521.
- A. Sanchez-Fernandez, T. Arnold, A. J. Jackson, S. L. Fussell, R. K. Heenan, R. A. Campbell and K. J. Edler, *Phys. Chem. Chem. Phys.*, 2016, **18**, 33240–33249.
- T. Arnold, A. J. Jackson, A. Sanchez-Fernandez, D. Magnone, A. E. Terry and K. J. Edler, *Langmuir*, 2015, **31**, 13894–13902.
- L. Sapir, C. B. Stanley and D. Harries, *The Journal of Physical Chemistry A*, 2016, **120**, 325.
- F. Merza, A. Fawzy, I. AlNashef, S. Al-Zuhair and H. Taher, *Energy Reports*, 2018, **4**, 77 – 83.
- R. Esquembre, J. Sanz, J. G. Wall, F. del Monte, C. R. Mateo and M. L. Ferrer, *Phys. Chem. Chem. Phys.*, 2013, **15**, 11248–11256.
- J. T. Gorke, F. Srienc and R. J. Kazlauskas, *Ionic Liquid Applications: Pharmaceuticals, Therapeutics, and Biotechnology*, American Chemical Society, 2010, vol. 1038, ch. 14, pp. 169–180.
- J. T. Gorke, F. Srienc and R. J. Kazlauskas, *Chem. Commun.*, 2008, 1235–1237.
- H. Monhemi, M. R. Housaindokht, A. A. Moosavi-Movahedi and M. R. Bozorgmehr, *Phys. Chem. Chem. Phys.*, 2014, **16**, 14882–14893.
- B.-P. Wu, Q. Wen, H. Xu and Z. Yang, *J. Mol. Catal. B: Enzym.*, 2014, **101**, 101–107.
- A. R. Harifi-Mood, R. Ghobadi and A. Divsalar, *Int. J. Biol. Macromol.*, 2017, **95**, 115–120.
- F. Milano, L. Giotta, M. R. Guascito, A. Agostiano, S. Sblendorio, L. Valli, F. M. Perna, L. Cicco, M. Trotta and V. Capriati, *ACS Sustain. Chem. Eng.*, 2017, **5**, 7768–7776.
- A. Sanchez-Fernandez, K. J. Edler, T. Arnold, D. Alba Venero and A. J. Jackson, *Phys. Chem. Chem. Phys.*, 2017, **19**, 8667–8670.
- S. Bryant, R. Atkin and G. G. Warr, *Langmuir*, 2017, **33**, 6878–6884.
- S. Bryant, R. Atkin and G. G. Warr, *Soft Matter*, 2016, **12**, 1645–1648.
- M. C. Gutiérrez, M. L. Ferrer, C. R. Mateo and F. del Monte, *Langmuir*, 2009, **25**, 5509–5515.
- H. Mohwald, *Annu. Rev. Phys. Chem.*, 1990, **41**, 441–476.
- S. Kewalramani, H. Hlaing, B. M. Ocko, I. Kuzmenko and M. Fukuto, *J. Phys. Chem.*, 2010, **1**, 489–495.
- G. van Rossum, *Python tutorial*, Technical Report CS-R9526, Centrum voor wiskunde en informatica (cwi) technical report, 1995.
- T. Kluyver, B. Ragan-Kelley, F. Pérez, B. Granger, M. Bussonnier, J. Frederic, K. Kelley, J. Hamrick, J. Grout, S. Corlay, P. Ivanov, D. Avila, S. Abdalla and C. Willing, Positioning and Power in Academic Publishing: Players, Agents and Agendas, 2016, pp. 87 – 90.
- A. Nelson, S. Prescott, I. Gresham and A. McCluskey, *refnx v0.0.15*, 2018.
- J. Goodman and J. Weare, *Comm App Math Comp Sci*, 2010, **5**, 65–80.
- D. Foreman-Mackey, D. W. Hogg, D. Lang and J. Goodman, *Publ. Astron. Soc. Pac.*, 2013, **125**, 306.
- T. Arnold, C. Nicklin, J. Rawle, J. Sutter, T. Bates, B. Nutter, G. McIntyre and M. Burt, *J. Synchrotron Rad.*, 2012, **19**, 408–416.
- T. Bayerl, R. Thomas, J. Penfold, A. Rennie and E. Sackmann, *Biophysical Journal*, 1990, **57**, 1095 – 1098.
- S. J. Johnson, T. M. Bayerl, W. Weihan, H. Noack, J. Penfold, R. K. Thomas, D. Kanellas, A. R. Rennie and E. Sackmann, *Biophys. J.*, 1991, **60**, 1017–1025.
- L. A. Clifton, M. Sanders, C. Kinane, T. Arnold, K. J. Edler,

- C. Neylon, R. J. Green and R. A. Frazier, *Phys. Chem. Chem. Phys.*, 2012, **14**, 13569–13579.
- 36 C. A. Helm, H. MÃ‰hwald, K. KjÃer and J. Als-Nielsen, *EPL (Europhysics Letters)*, 1987, **4**, 697.
- 37 J. Daillant, L. Bosio and J. J. Benattar, *EPL (Europhysics Letters)*, 1990, **12**, 715.
- 38 R. S. Armen, O. D. Uitto and S. E. Feller, *Biophysical Journal*, 1998, **75**, 734 – 744.
- 39 H. I. Petracche, S. E. Feller and J. F. Nagle, *Biophys. J.*, 1997, **72**, 2237–2242.
- 40 W. J. Sun, R. M. Suter, M. A. Knewton, C. R. Worthington, S. Tristram-Nagle, R. Zhang and J. F. Nagle, *Phys. Rev. E*, 1994, **49**, 4665–4676.
- 41 A. Tardieu, V. Luzzati and F. C. Reman, *J. Mol. Biol.*, 1973, **75**, 711–733.
- 42 N. Kučerka, M. A. Kiselev and P. Balgavý, *Eur. Biophys. J.*, 2004, **33**, 328–334.
- 43 J. F. Nagle and D. A. Wilkinson, *Biophys. J.*, 1978, **23**, 159–175.
- 44 G. Schmidt and W. Knoll, *Berichte der Bunsengesellschaft fÃ¼r physikalische Chemie*, 1985, **89**, 36–43.
- 45 J. Pan, F. A. Heberle, S. Tristram-Nagle, M. Szymanski, M. Koepfinger, J. Katsaras and N. Kučerka, *Biochimica et biophysica acta*, 2012, **1818**, 2135â€”2148.
- 46 F. Abelès, *J. Phys. Radium*, 1950, **11**, 307–309.
- 47 L. G. Parratt, *Phys. Rev.*, 1954, **95**, 359–369.
- 48 C. Tanford, *The Hydrophobic Effect: Formation of Micelles and Biological Membranes*, John Wiley & Sons Ltd., 2nd edn, 1980.
- 49 D. Vaknin, K. Kjaer, J. Als-Nielsen and M. LÃ¶nsche, *Biophys. J.*, 1991, **59**, 1325–1332.
- 50 G. A. Lawrie, K. A. Gunton, G. T. Barnes and I. R. Gentle, *Colloids Surf. A*, 2000, **168**, 13–25.